A Single Amino Acid at Residue 188 of the Hexon Protein Is Responsible for the Pathogenicity of the Emerging Novel Virus Fowl Adenovirus 4

Yu Zhang,[a] Aijing Liu,[a] Yanan Wang,[a] Hongyu Cui,[a] Yulong Gao,[a] Xiaole Qi,[a] Changjun Liu,[a] Yanping Zhang,[a] Kai Li,[a] Li Gao,[a] Qing Pan,[a] Xiaomei Wang[a,b]

[a]State Key Laboratory of Veterinary Biotechnology, Harbin Veterinary Research Institute, Chinese Academy of Agricultural Sciences, Harbin, China
[b]Jiangsu Co-innovation Center for the Prevention and Control of Important Animal Infectious Diseases and Zoonoses, Yangzhou University, Yangzhou, China

ABSTRACT Since 2015, severe hydropericardium-hepatitis syndrome (HHS) associated with a novel fowl adenovirus 4 (FAdV-4) has emerged in China, representing a new challenge for the poultry industry. Although various highly pathogenic FAdV-4 strains have been isolated, the virulence factor and the pathogenesis of novel FAdV-4 are unclear. In our previous studies, we reported that a large genomic deletion (1,966 bp) is not related to increased virulence. Here, two recombinant chimeric viruses, rHN20 strain and rFB2 strain, were generated from a highly pathogenic FAdV-4 strain by replacing the *hexon* or *fiber-2* gene of a nonpathogenic FAdV-4, respectively. Both chimeric strains showed similar titers to the wild-type strain *in vitro*. Notably, rFB2 and the wild-type strain induced 100% mortality, while no mortality or clinical signs appeared in chickens inoculated with rHN20, indicating that hexon, but not fiber-2, determines the novel FAdV-4 virulence. Furthermore, an R188I mutation in the hexon protein identified residue 188 as the key amino acid for the reduced pathogenicity. The rR188I mutant strain was significantly neutralized by chicken serum *in vitro* and *in vivo*, whereas the wild-type strain was able to replicate efficiently. Finally, the immunogenicity of the rescued rR188I was investigated. Nonpathogenic rR188I provided full protection against lethal FAdV-4 challenge. Collectively, these findings provide an in-depth understanding of the molecular basis of novel FAdV-4 pathogenicity and present rR188I as a potential live attenuated vaccine candidate or a novel vaccine vector for HHS vaccines.

IMPORTANCE HHS associated with a novel FAdV-4 infection in chickens has caused huge economic losses to the poultry industry in China since 2015. The molecular basis for the increased virulence remains largely unknown. Here, we demonstrate that the hexon gene is vital for FAdV-4 pathogenicity. Furthermore, we show that the amino acid residue at position 188 of the hexon protein is responsible for pathogenicity. Importantly, the rR188I mutant strain was neutralized by chicken serum *in vitro* and *in vivo*, whereas the wild-type strain was not. Further, the rR188I mutant strain provided complete protection against FAdV-4 challenge. Our results provide a molecular basis of the increased virulence of novel FAdV-4. We propose that the rR188I mutant is a potential live attenuated vaccine against HHS and a new vaccine vector for HHS-combined vaccines.

KEYWORDS fowl adenovirus 4, virulence, hexon, pathogenesis, vaccine development

Fowl adenoviruses (FAdVs) belong to the *Aviadenovirus* genus and the *Adenoviridae* family. FAdVs are further classified into five species (designated FAdV-A to -E) based on molecular criteria and enzyme digestion patterns or 12 serotypes based on serum cross-neutralization tests (designated FAdV-1 to -7, -8a, -8b, and -9 to -11) (1, 2). FAdV-

Address correspondence to Qing Pan, panqing20050101@126.com, or Xiaomei Wang, wangxiaomei@caas.cn.

4 infection was first reported in Pakistan in 1987. Subsequent outbreaks have been reported around the world, resulting in significant economic losses for the poultry industry (3). Pathogenic FAdV strains associated with hydropericardium-hepatitis syndrome (HHS) (4, 5), inclusion body hepatitis (IBH) (6–8), and gizzard erosion (9–11) have been isolated; therefore, diagnostic methods and vaccines for these strains are in development. Some nonpathogenic strains were identified and developed into vaccine vectors, such as CELO (12–14), a FAdV-1 strain.

Notably, severe HHS caused by a highly pathogenic FAdV has emerged in chickens, ducks, and geese in China since 2015, with mortality rates from 20 to 100% (15–19). The causative agent for this HHS was identified as FAdV-4, which was identified as a novel FAdV-4 because of a large genomic deletion (1,966 bp) between *ORF42* and *ORF43* (16, 20, 21). In previous studies, we developed a reverse genetic platform for FAdV-4 and reported that the large genomic deletion is unrelated to increased virulence (22). Although identifying the molecular basis of the increased virulence is important for in-depth understanding of pathogenicity and pathogenesis, genes that cause increased virulence in the emerging FAdV-4 are not well known (23).

Identifying virulence genes is critical for disease control and vaccine development. Recently, the spike (S) gene of the emerging SARS-CoV-2 was defined to play critical roles for virulence, which provided important information for understanding pathogenesis and enabled the development of novel therapeutic antibodies and vaccines (24–26). The *meq* gene of *Marek's disease virus* was identified as the virulence gene (27, 28). Using these findings, a live attenuated vaccine was developed that showed efficient protection for Marek's disease (29, 30). The live attenuated strain was further explored as a vaccine vector for combined vaccines of other avian diseases. Several studies have attempted to identify the potential gene function of the novel FAdV-4. Short fiber-1 was defined as the key factor for triggering infection by FAdV-4 by directly binding to the coxsackievirus and adenovirus receptor (CAR) (31, 32). Deleting the full-length or N-terminal sequence of fiber-2 reduced virulence by reducing replication ability or destroying viral structure (33, 34). Fiber-1 and penton were independent of increased virulence (35). Although the hexon and fiber-2 genes are associated with pathogenic CH/HNJZ/2015 strain's virulence (36), the roles of these two genes in other virulent strains and their exact locations remain unknown.

In this study, the hexon gene, but not fiber-2, was identified as the critical virulence gene for FAdV-4. A single amino acid at position 188 of the hexon protein was further identified as the determinant for FAdV-4 pathogenicity. We first identified the molecular basis for the increasing virulence of the emerging novel FAdV-4. The R188I mutant strain, rR188I, can replicate as well as the wild-type strain *in vitro* but is totally nonpathogenic by serum neutralization *in vivo*. Furthermore, the rR188I strain is nonpathogenic and provides full protection against HHS, thus highlighting its potential value for development as a live attenuated vaccine or combined vaccine vector.

RESULTS

Hexon, not fiber-2, determines novel FAdV-4 pathogenicity. To identify the virulence genes of the HLJFAd15 strain, rHN20 and rFB2 chimeric viruses were generated by replacing the hexon or fiber-2 gene of the HLJFAd15 strain with hexon or fiber-2 from the nonpathogenic strain ON1, respectively (Fig. 1A). The replication capacity of the two chimeric recombinant viruses in leghorn male hepatocellular (LMH) cells was not different from that of the rescued wild-type virus (rWT-FAdV4) (Fig. 1B).

The pathogenicity of rHN20 and rFB2 was tested on 3-week-old specific-pathogen-free (SPF) chickens. Unexpectedly, the chickens in the rHN20 and mock control groups did not show any symptoms until the end of the experiment, whereas all the chickens in the rFB2 and rWT-FAdV4 groups died within 4 days after challenge (Fig. 1C). The heart, liver, spleen, lung, kidney, thymus, and bursa tissues were collected from dead or euthanized chickens for viral load titration. The viral load in the rFB2 and rWT-FAdV4 groups in each tissue was not significantly different. The viral distribution was the
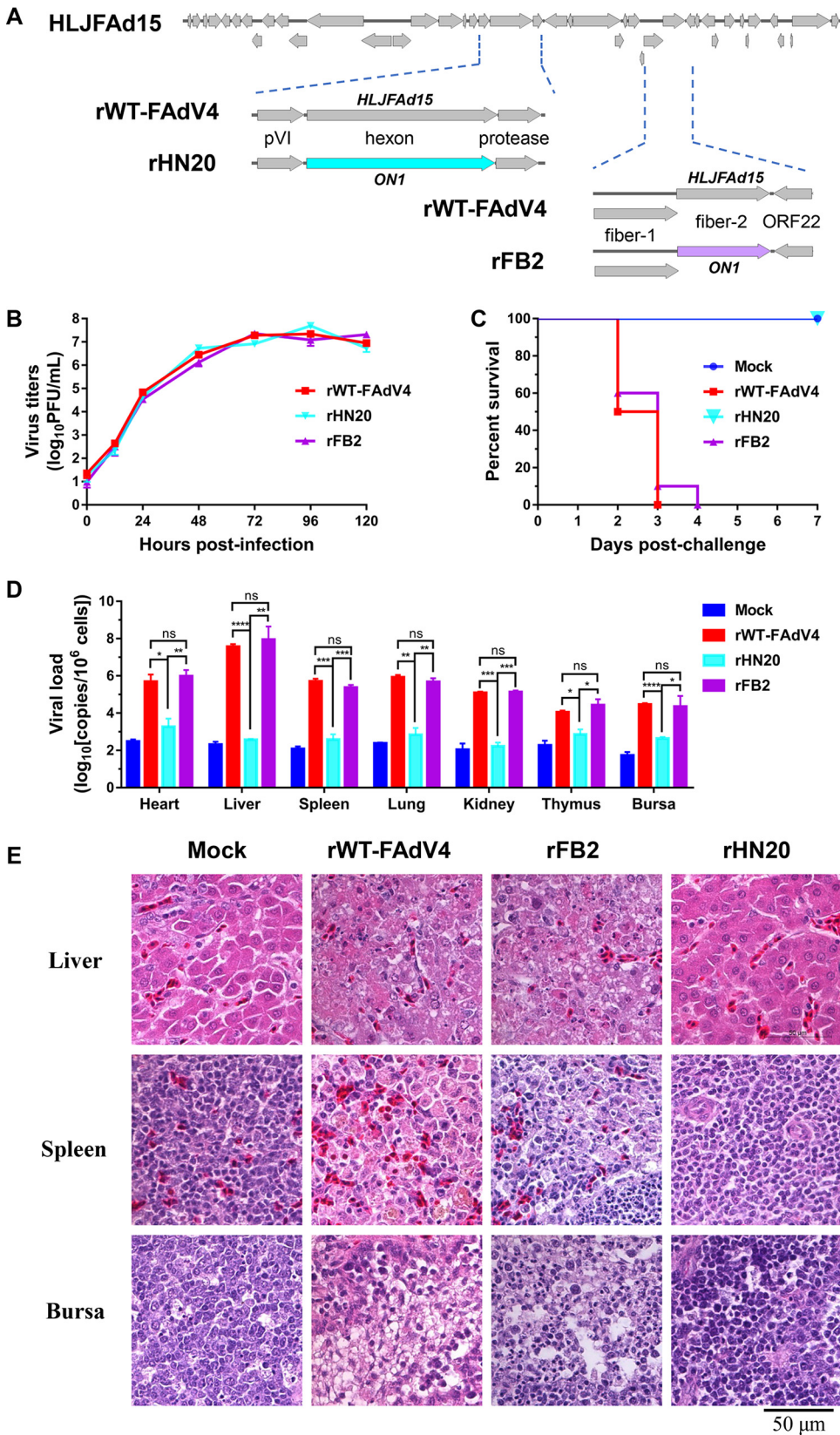
FIG 1 Hexon, not fiber-2, determines novel FAdV-4 pathogenicity. (A) Schematic of fiber-2 and hexon gene replacement recombinant virus generation based on the FAdV-4 HLJFAd15 strain fosmid infectious clone. (B) Virus growth kinetics. LMH cells were infected with rWT-FAdV4, rHN20, and rFB2 at an MOI of 0.01. At each

(Continued on next page)

highest in the liver. The viral loads of rFB2 and rWT-FAdV4 were significantly higher than that of rHN20 and mock controls, and the rHN20 group presented a low viral load in various tissues (Fig. 1D). Gross autopsy of chickens infected with rWT-FAdV4 or rFB2 showed a swollen and friable liver or hydropericardium, as previously reported (21; data not shown). Moreover, pathological histology analysis of the liver, spleen, and bursa tissues showed that rWT-FAdV4 or rFB2 infection caused severe pathological necrosis. No significant lesions were observed in the rHN20 and mock infection groups (Fig. 1E).

Collectively, our data demonstrate that hexon, not fiber-2, determines the pathogenicity of novel FAdV-4.

R188I mutation plays a critical role in FAdV-4 attenuation. Based on the hexon amino acid sequences, evolutionary analysis and sequence alignment of ON1 and 16 novel FAdV-4 strains isolated in China since 2015 were performed. The results showed that the hexon proteins of virulent epidemic strains were all in the same branch and shared the same amino acid sequence as that of HLJFAd15 (Fig. 2A), but there were 13 amino acid differences compared to the nonpathogenic strain ON1 (Fig. 2B). To investigate the contribution of individual amino acids in the hexon protein to FAdV-4 pathogenicity, 13 single-amino acid mutant viruses (designated rS164T, rR188I, rR193Q, rQ195E, rN238D, rT240A, rN243E, rI263M, rV264I, rA410T, rI574V, rP797A, and rA842G) were generated (Fig. 2B) and used to test the pathogenicity of the mutant viruses in 4-week-old SPF chickens. Surprisingly, chickens infected with rR188I, like rHN20, did not die or develop any clinical signs. Chickens infected with the other mutant viruses all died within 1 to 4 days after challenge (100% mortality rate) (Fig. 2C and D). Correspondingly, rR188I and rHN20 copy numbers were similar to the background value of the mock group, whereas the other groups had high viral loads in the liver (Fig. 2E). These results indicate that the loss of virulence from the rHN20 strain results from an arginine (R)-to-isoleucine (I) substitution at amino acid 188 of the hexon protein (R188I). Virulence is not related to the other 12 differential amino acids.

I188R mutation confers rHN20 virulence. To further assess the role of R188 in FAdV-4 pathogenicity, we made a reverse I188R mutation in the nonpathogenic strain rHN20, resulting in the rI188R recombinant virus (Fig. 3A). The virus growth kinetics showed that I188R had the same replication ability as rWT-FAdV4, rHN20, and R188I in LMH cells (Fig. 3B). Challenge of SPF chickens with these four viruses resulted in 100% death for rWT-FAdV4- and rI188R-infected chickens but not in rHN20- and rR188I-infected chickens, as expected (Fig. 3C). No other clinical symptoms were observed in the rHN20 and rR188I groups. Moreover, the livers of dead or euthanized chickens infected with rWT-FAdV4 or rI188R contained high viral loads, whereas the rHN20 and R188I groups had very low viral loads (Fig. 3D). In addition, pathological observation showed that the rWT-FAdV4 and rI188R groups presented severe IBH and hepatocellular injury, whereas rHN20- and rR188I-infected chickens were not different from healthy chickens (Fig. 3E). These data demonstrate that the I188R mutation confers rHN20 virulence, and amino acid 188 of the hexon protein determines the FAdV-4 virulence.

Phylogenetic and amino acid 188 conservation analysis of hexon from different FAdV-4 isolates. To further analyze the role of amino acid 188 of hexon in the pathogenicity of other FAdV-4 isolates, we downloaded the complete hexon sequences of all reported naturally nonpathogenic strains (ON1, KR5, and B1-7) and foreign pathogenic strains (Mx-SHP95 and AG234-CORR) from GenBank and compared these sequences to that of novel FAdV-4. As previously reported, pathogenic novel FAdV-4 is on a unique

FIG 1 Legend (Continued)
time point, viruses were harvested and quantified using a plaque assay. (C) Survival curve of 3-week-old SPF chickens after challenge with rWT-FAdV4, rHN20, and rFB2 ($n = 10$). (D) Viral loads in different tissues. The heart, liver, spleen, lung, kidney, thymus, and bursa tissues from each group were collected at the end of the experiment ($n = 3$). Viral DNA was detected using TaqMan quantitative real-time PCR. Error bars represent the standard errors of the mean (SEM). *, $P < 0.05$; **, $P < 0.01$; ***, $P < 0.001$; ns, not significant. (E) Histological examination of the liver, spleen, and bursa from chickens infected with rWT-FAdV4, rHN20, and rFB2. Scale bar, 50 μm.
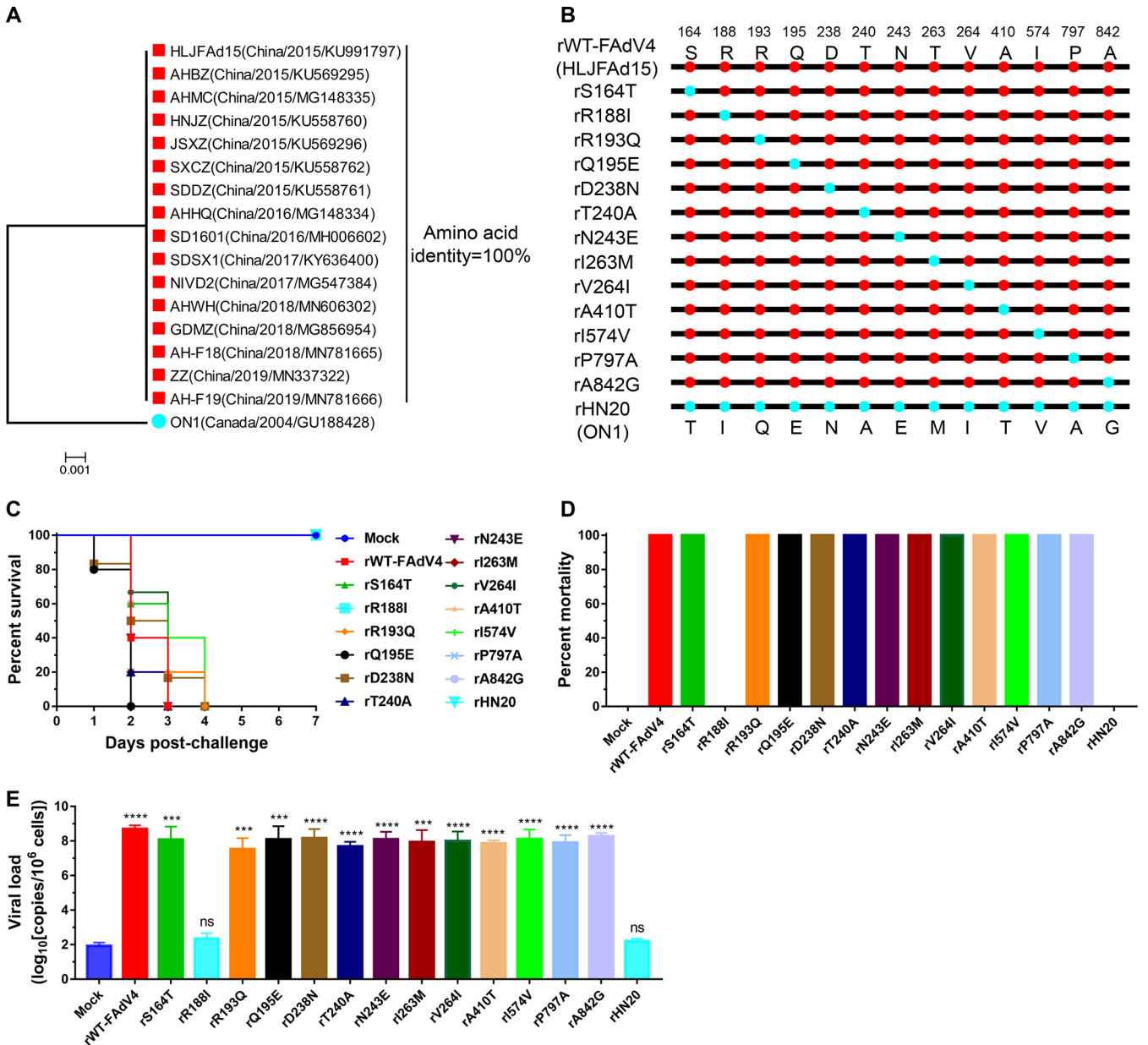
FIG 2 rR188I mutation reduces FAdV-4 virulence in SPF chickens. (A) Phylogenetic analysis based on the hexon amino acid sequences. GenBank accession numbers and time periods and geographical regions of virus isolation are indicated in parentheses. Red square, novel FAdV-4 strain; light blue circle, nonpathogenic ON1 strain. (B) Schematic of the generation of mutant viruses. Thirteen amino acids of the rWT-FAdV4 (HLJFAd15) strain hexon protein that were different from the ON1 strain were mutated to the residues of ON1, respectively. The diagrams are not to scale. (C) Survival curve. Thirteen single-amino-acid mutant viruses were injected into 3-week-old SPF chickens. rWT-FAdV-4, rHN20, and mock-injected chickens (control) were the three groups ($n = 5$). (D) Survival rates after viral challenge. (E) Viral load in the liver in different groups ($n = 3$). Error bars represent the SEM. *, $P < 0.05$; **, $P < 0.01$; ***, $P < 0.001$; ns, not significant.

evolutionary branch (16), but the nonpathogenic B1-7, KR5, and ON1 strains are located on different evolutionary branches (Fig. 4A). Interestingly, independent of time period and geographical region, amino acid 188 of hexon is R in all the pathogenic strains, while the nonpathogenic strains contain I (Fig. 4B). These alignment results further suggest that amino acid 188 of hexon determines FAdV-4 pathogenicity.

Nonpathogenic strains have limited ability to infect hepatocytes *in vivo*. The data presented above suggest that FAdV-4 pathogenicity may correlate with the ability to infect the liver *in vivo* because pathogenic strains caused higher viral loads in the liver but nonpathogenic strains did not (Fig. 1D, 2E, and 3D). To evaluate the real-time infection ability of different strains on the liver *in vivo*, we monitored the liver viral load
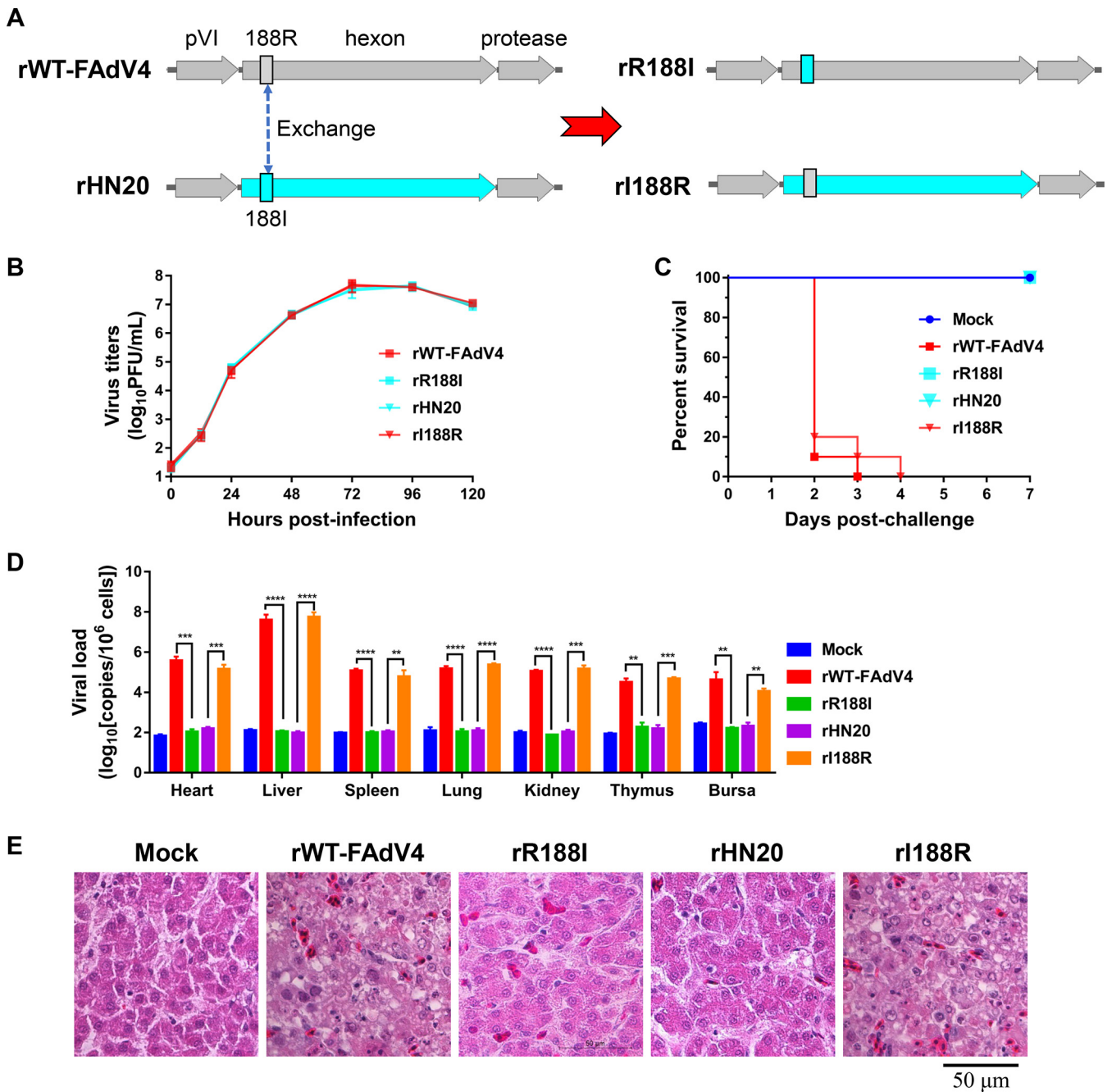
FIG 3 rI188R mutation confers rHN20 virulence in SPF chickens. (A) Detailed schematic representation of the four recombinant viruses. rWT-FAdV4, rescued wild type FAdV-4; rHN20, the hexon gene was replaced with the ON1 sequence; rI188R, amino acid 188 of the hexon protein from the rHN20 strain was reverse mutated to wild type; rR188I, amino acid 188 of the hexon protein of the rWT-FAdV4 strain was mutated to the ON1 sequence. (B) Virus growth curves of the four viruses in LMH cells. (C) Survival curve. The four viruses were intramuscularly injected into 3-week-old SPF chickens ($n = 10$). (D) Viral load in the liver in different groups ($n = 3$). Error bars represent the SEM. *, $P < 0.05$; **, $P < 0.01$; ***, $P < 0.001$; ns, not significant. (E) Histological examination of the liver, spleen, and bursa. Scale bar, 50 μm.

at different time points after intramuscular injection of these viruses (Fig. 5A). The data showed that rHN20 and rR188I infected significantly fewer hepatocytes *in vivo* than did rWT-FAdV4 and rI188R (Fig. 5A). However, when primary chicken embryo liver (CEL) cells were infected with these viruses, the viral genome content was not different (Fig. 5B). In addition, there was no difference in the ability of these viruses to infect LMH cells (Fig. 3B). These data demonstrate that both pathogenic and nonpathogenic strains have the same ability to infect hepatocytes but that nonpathogenic strains cannot infect the liver with high efficiency *in vivo*.
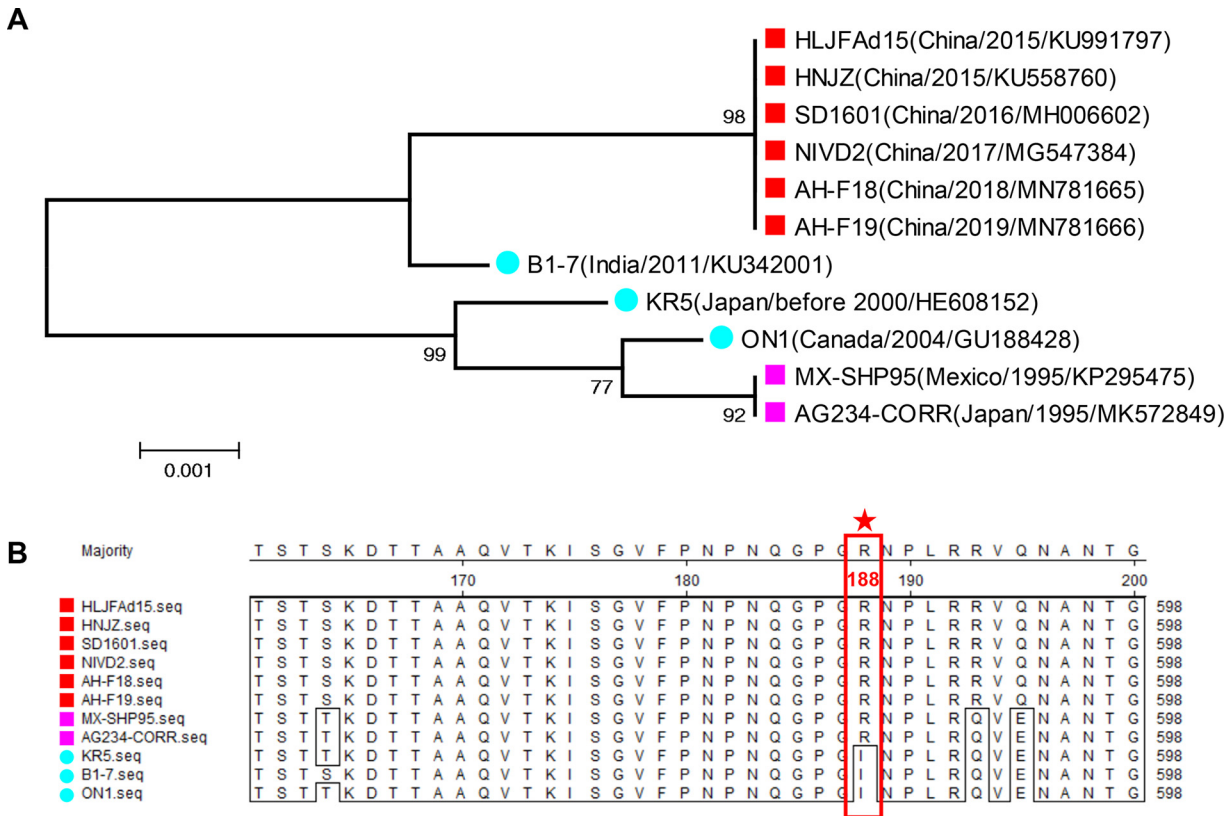
FIG 4 Phylogenetic and hexon amino acid 188 conservation analysis of different FAdV-4 isolates. (A) Phylogenetic tree based on hexon. GenBank accession numbers and time periods and geographical regions of virus isolation are indicated in parentheses. Red square, novel pathogenic FAdV-4 strain; purple squares, foreign pathogenic strains; light blue circle, nonpathogenic strain. (B) Sequence alignment analysis for hexon amino acid 188 from different FAdV-4 isolates. The red star highlights amino acid 188.

Considering that passage through the blood is required before viral entry into the target tissues, we injected these viruses intravenously and examined the viral loads in the blood, liver, and kidney. Both of the pathogenic strains proliferated with high efficiency in the blood, whereas effective proliferations of nonpathogenic strains were not detectable (Fig. 5C). We further examined the viral load in the liver and kidney at 24 h postinfection and observed that rHN20 and rR188I loads were significantly lower than rWT-FAdV4 and rI188R loads (Fig. 5D). Taken together, four viruses showed similar ability to infect hepatocytes *in vitro*, while the pathogenic rWT-FAdV4 and rI188R were capable to induce greater viremia and higher virus loads in target tissues *in vivo*.

Hexon amino acid 188 determines the neutralization capacity of SPF chicken serum against FAdV-4. To demonstrate that the blood has differential effects on FAdV-4 pathogenic and nonpathogenic strains, rWT-FAdV4 and rHN20 EGFP reporter viruses were preincubated with fresh SPF chicken serum for 1 h at 42°C before infecting LMH cells. Fluorescence microscopy and flow cytometry showed that the infectivity of rWT-EGFP in LMH cells was not significantly affected by SPF chicken serum, whereas rHN20-EGFP was significantly neutralized. In addition, the extent of neutralization was positively correlated with the serum concentration (Fig. 6A and B). These results show that SPF chicken serum neutralizes nonpathogenic strains with high efficiency.

To further demonstrate the relationship of amino acid 188 with serum-neutralized viruses, the four viruses were simultaneously pretreated with SPF chicken serum or serum-free medium and used to infect LMH cells. We observed that treatment with serum significantly inhibited the cytopathic effect (CPE) of rHN20 and rR188I but had no effect on rWT-FAdV4 and rI188R (Fig. 6C). Correspondingly, the viral loads in serum-pretreated rHN20- and rR188I-infected LMH cells were significantly lower than that in medium-pretreated cells, but serum treatment did not reduce viral loads in rWT-FAdV4- and rI188R-infected LMH cells
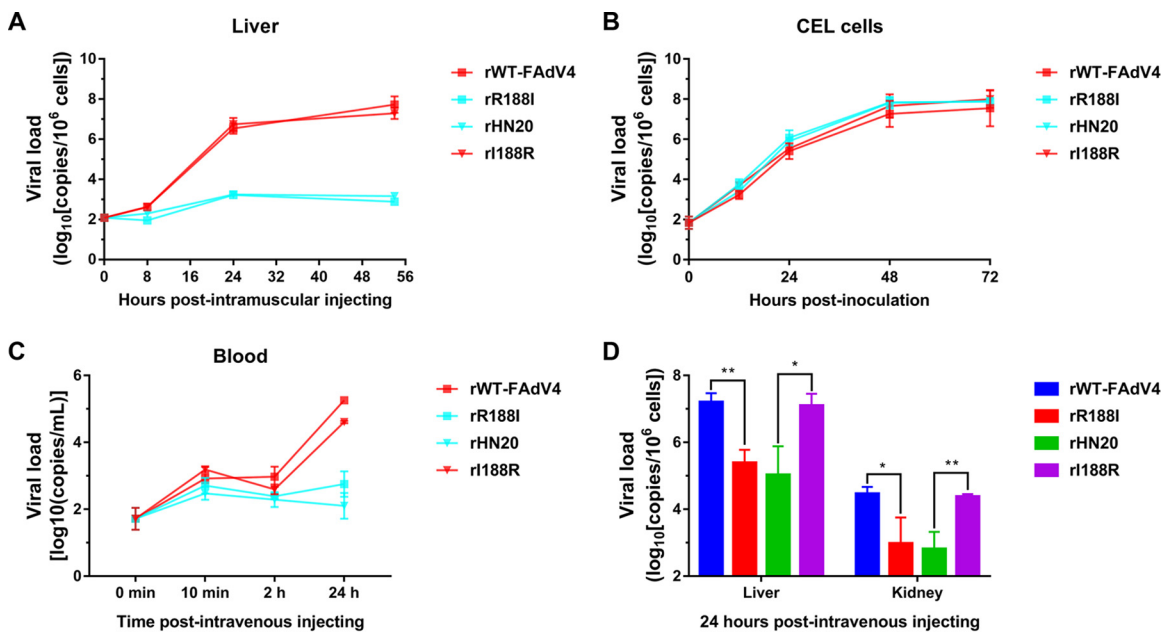
FIG 5 Characteristics of the recombinant viruses infecting hepatocytes *in vivo* and *in vitro*. (A) Three-week-old SPF chickens were intramuscularly injected with rWT-FAdV4, rHN20, rI188R, and rR188I ($n = 10$, dose $= 10^4$ PFU). The livers were collected, and viral loads were evaluated using TaqMan quantitative real-time PCR at the indicated time points ($n = 3$). (B) CEL cells were infected with rWT-FAdV4, rHN20, rI188R, and rR188I at an MOI of 0.01. At each indicated time point, the cells were harvested, and the viral loads were analyzed using TaqMan quantitative real-time PCR ($n = 3$). (C and D) Three-week-old SPF chickens were intravenously injected with rWT-FAdV4, rHN20, rI188R, and rR188I ($n = 3$, dose $= 10^6$ PFU). (C) Viral loads in the blood at different time points. (D) Viral loads in the liver and kidney at 24 h postinjection. Error bars represent the SEM. *, $P < 0.05$; **, $P < 0.01$; ***, $P < 0.001$; ns, not significant.

(Fig. 6D). Together, these results demonstrate that SPF chicken serum neutralizes rHN20- and rR188I-mediated hepatocyte infection.

rR188I mutation provides efficient protection against FAdV-4 challenge. Because rR188I is a nonpathogenic recombinant virus with only 1 amino acid substitution compared to wild-type FAdV-4, we hypothesized that rR188I confers immunogenicity. To assess whether the rR188I mutation has the potential for live attenuated vaccines, 2-week-old SPF chickens were inoculated with rR188I. Fourteen days later, chickens were challenged with a lethal dose of rWT-FAdV4 and observed for morbidity and mortality. The chickens in the challenge control group exhibited lethargy and piloerection. Death began at 2 days postchallenge and reached 100% mortality at 5 days postchallenge. However, neither death nor clinical symptoms occurred in the rR188I group or the healthy control group during 14 days (Fig. 7A). The heart, liver, spleen, lung, kidney, thymus, and bursa tissues from chickens at 5 days postchallenge were collected, and viral loads were determined. Viral loads in the rR188I and healthy control groups were not significantly different but were much lower than that in the challenge control group. In the challenge control group, the highest viral load was seen in the liver, reaching 107 to 108 copies per million cells (Fig. 7B). Correspondingly, severe pathological tissue damage was seen in different tissues of the challenge control group. The liver cells showed degenerative necrosis and inflammatory cell infiltration concurrent with generalized lymphocytic necrosis and reduction with giant cell hyperplasia in the spleen and bursa. No histopathological symptoms were observed in the rR188I or healthy control groups (Fig. 7C). These data demonstrate that rR188I provides efficient protection against FAdV-4 challenge.

DISCUSSION

HHS associated with a novel FAdV-4 infection in chickens has caused huge economic losses to the poultry industry in China since 2015. The FAdV-4 genome is comprised of approximately 43- to 45-kb double-stranded DNA encoding more than 40
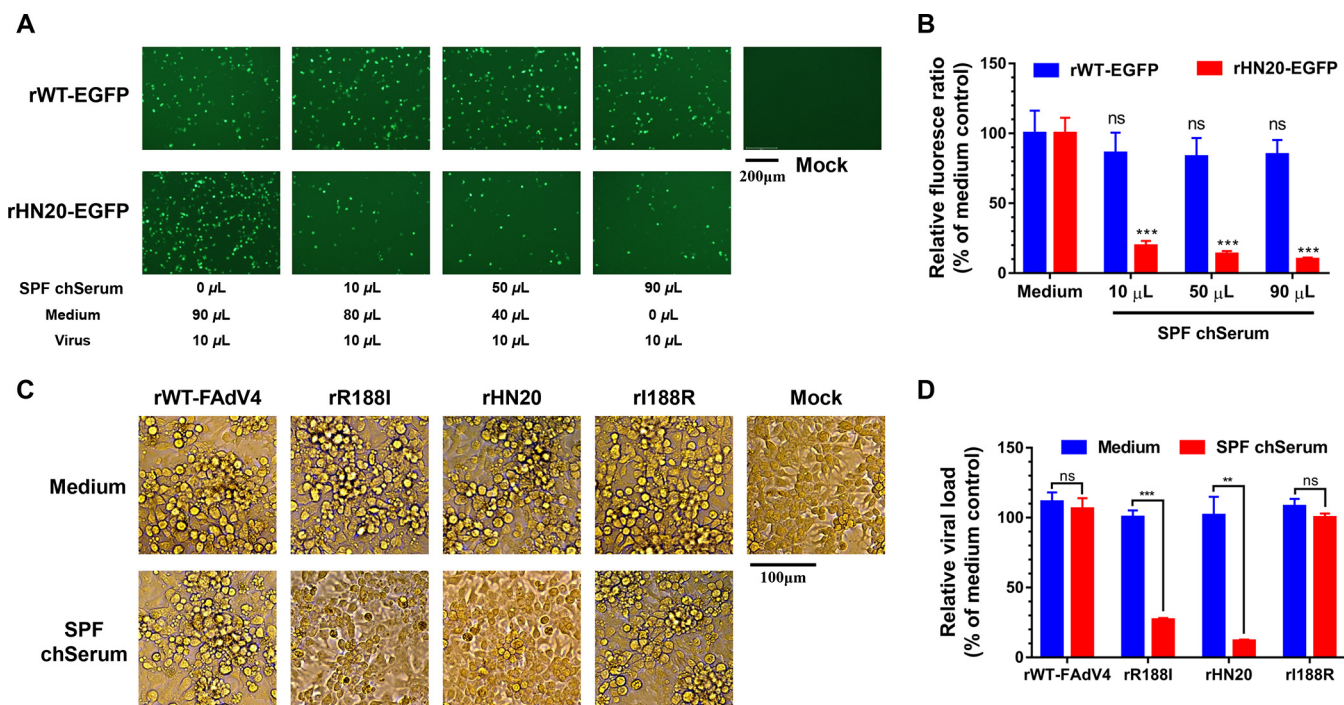
FIG 6 Neutralization potency of SPF chicken serum against each recombinant virus. (A and B) Effect of SPF chicken serum concentration on rWT-EGFP and rHN20-EGFP infection of LMH cells. The rWT-EGFP or rHN20-EGFP viruses were incubated for 1 h at 42°C with the indicated various amounts of fresh 3-week-old SPF chicken serum. The viruses were then incubated with LMH cells for 1 h. The medium was replaced, and the cells were cultured for another 48 h. (A) Cells were examined using fluorescence microscopy. Scale bar, 200 μm. (B) The relative ratio of fluorescent cells was detected using flow cytometry and normalized to the medium-only control (n = 3). (C and D) Neutralization of rWT-FAdV4, rHN20, rI188R, and rR188I by SPF chicken serum. The four strains were incubated for 1 h at 42°C with 90% fresh serum or medium. The viruses were used to infect LMH cells for 48 h. (C) The CPE was examined using microscopy. Scale bar, 100 μm. (D) Viral loads were detected and normalized to medium-only controls (n = 3). Error bars represent the SEM. *, $P < 0.05$; **, $P < 0.01$; ***, $P < 0.001$; ns, not significant.

proteins. However, the virulence genes and their locations are poorly understood. Investigating the dominant virulence gene is critical for understanding pathogenesis and enabling vaccine development. Identifying the SARS-CoV-2 spike gene (24, 37), the influenza virus PB2 gene (38), and nonstructural genes of the Zika virus (39) clarified the pathogenic mechanisms and highlighted novel insights for vaccine development. Our previous studies reported that a natural large genomic deletion was unrelated to the increased virulence of novel FAdV-4 (22). Further, we showed that fiber-1 protein mediates virus adsorption to cellular receptors (31, 32). Recently, attention has been focused on the molecular basis of the increased virulence of the highly pathogenic FAdV-4. In the present study, the capsid protein-encoding gene, hexon, but not fiber-2, was identified as the dominant virulence gene of novel FAdV-4. These findings contrast previous reports that hexon and fiber-2 genes are closely associated with the virulence of novel FAdV-4. Consequently, the hexon gene was identified as the critical virulence gene underlying the increasing virulence of all novel FAdV-4 strains, whereas fiber-2 activity is limited to specific strains.

Virulence based on a single amino acid often appears in RNA viruses but is rarely reported in DNA viruses. Amino acid 367 of the Tembusu virus E protein plays a critical role in pathogenesis (40), and amino acid 431 of the H1N1 swine influenza virus (SIV) PB2 protein determines its virulence in mice (41). Here, we report that the single amino acid R188 of the hexon protein is responsible for novel FAdV-4 pathogenicity. All chickens survived and showed no clinical symptoms when inoculated with a lethal dose of the rescued mutant strain rR188I. Inducing an R188I mutation totally decreased the pathogenicity of FAdV-4 in vivo and showed no impact for virus replication in vitro. Moreover, the FAdV-4 hexon sequences were aligned with those of three reported natural nonpathogenic FAdV-4 strains (ON1, KR5, and B1-7), which have a conserved isoleucine at position 188. In contrast, arginine is present at this position in all pathogenic
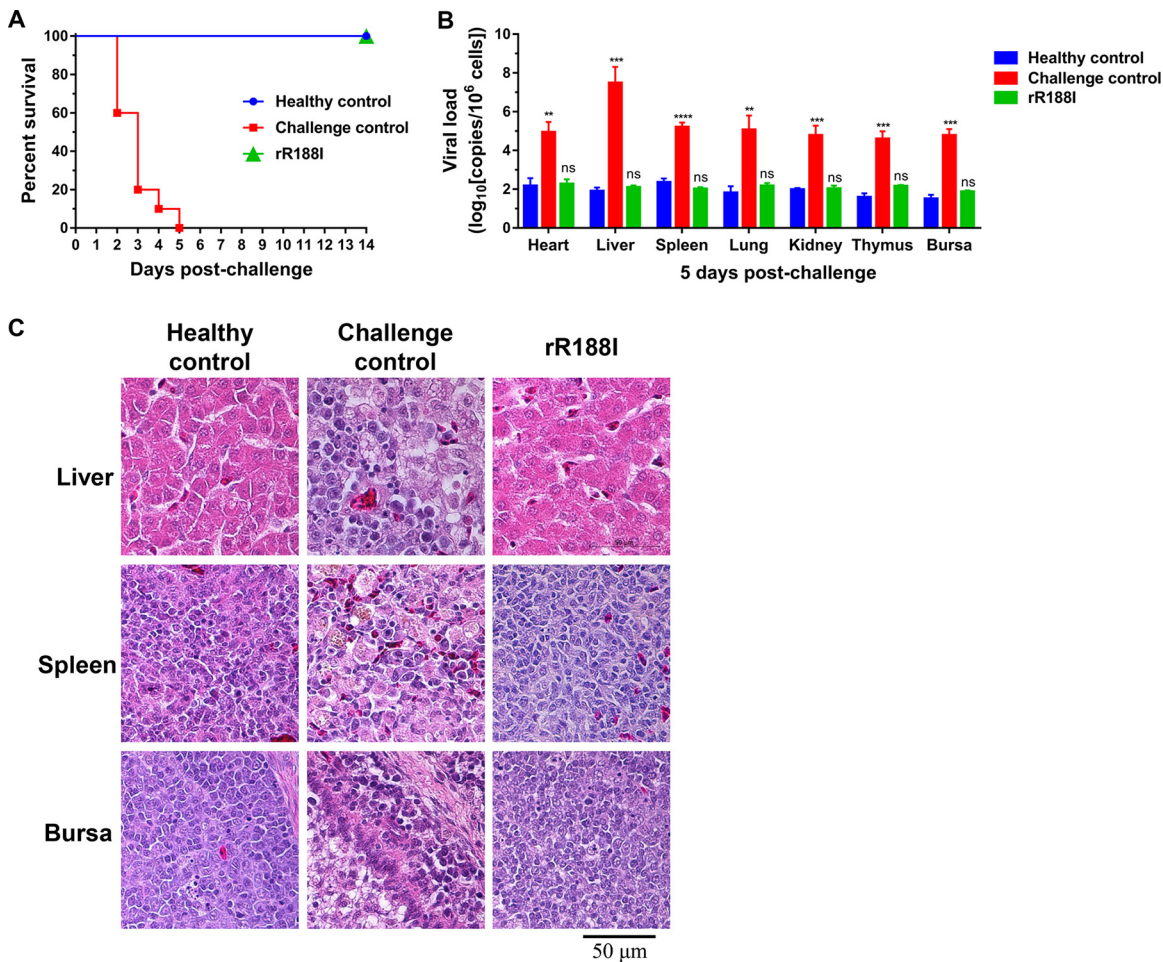
FIG 7 rR188I provides full protection against FAdV-4 challenge. (A) Survival curve. Two-week-old SPF chickens were inoculated with rR188I or DMEM/F12 medium ($n = 10$). At 2 weeks after immunization, chickens were challenged with rWT-FAdV4. The healthy control group did not receive any treatment. (B) Viral loads of different tissues in different groups at 5 days postchallenge. The heart, liver, spleen, lung, kidney, thymus, and bursa tissues from each group were collected. Viral DNA was detected using TaqMan quantitative real-time PCR. Error bars represent the SEM. *, $P < 0.05$; **, $P < 0.01$; ***, $P < 0.001$; ns, not significant. (C) Histological examination of the liver, spleen, and bursa from different groups. Scale bar, $50\,\mu m$.

FAdV-4 strains, regardless of time period and geographical region. The alignment results further strengthened the conclusion that R188 of the hexon protein is the virulence determinant of novel FAdV-4. These findings highlight the molecular basis for the increasing virulence of novel FAdV-4. Further, this is the first report of a single amino acid changing the virulence of an adenovirus, which is valuable for in-depth understanding of the virulence evolution of DNA viruses, especially adenoviruses.

As reported previously, human adenovirus 5 (HAdV-5) has a higher viral load in the liver compared to other tissues, and its hexon protein is the critical determinant for HAdV-5 infecting liver cells (42, 43). A single amino acid mutation (T425A) in hexon greatly reduced HAdV-5 infection in liver tissue in mice (44). We showed that the hexon protein is the pathogenicity determinant of novel FAdV-4, but the molecular basis remains unclear. Novel FAdV-4 infected various organs in chickens, with the highest viral load in the liver, where it induced severe IBH. However, the hexon replacement strain rHN20 and the R188I mutant strain rR188I did not effectively replicate in the liver or other tissues *in vivo*, although both nonpathogenic strains replicated similarly to the wild-type pathogenic strain *in vitro*. To further investigate this potential mechanism, four strains were directly inoculated into the blood. rHN20 and rR188I infections in the liver were significantly neutralized by the serum, with similar results in LMH cells *in vitro*. The pathogenic FAdV-4 was transported effectively from the blood to the liver,

whereas the nonpathogenic strains were neutralized by the serum because of the R188I mutant. This is the first report that a single amino acid mutant R188I of the hexon protein is responsible for reduced FAdV-4 pathogenicity. The R188I mutant may facilitate the innate immune system or complement system activation to neutralize nonpathogenic FAdV-4 (44–46). However, the mechanism of virus neutralization needs further investigation.

Adenovirus vectors are widely developed and used for novel vaccine development, such as HAdV-5 vector-based SARS-CoV-2 (47), Ebola (48), and Zika (49) vaccines. For FAdVs, the nonpathogenic strain CELO (FAdV-1) was first developed as a vector carrying cDNA encoding avian infectious bursal disease virus proteins (13, 14). However, FAdV-4 is the most pathogenic of 12 FAdV serotypes, and CELO-based vaccines cannot provide full protection against FAdV-4 infection. Here, the artificial rescue strain rR188I protected chickens against FAdV-4 challenge when rR188I was used as a live vaccine. In addition, rR188I is valuable as a vector for delivering other exogenous immunogenic proteins. Combined live vaccines containing rR188I may prevent emerging HHS and exogenous protein-related disease.

In summary, the molecular underpinnings of the increased virulence of novel FAdV-4 were first described in this study. The hexon gene, but not the fiber-2 gene, was identified as the critical FAdV-4 virulence gene, and a single amino acid at position 188 of the hexon protein determines pathogenicity. The pathogenic FAdV-4 was transported from the blood to the liver, whereas the nonpathogenic strains, including the R188I mutant, were neutralized in the serum. Furthermore, the rR188I strain was totally nonpathogenic and provided full protection against HHS, highlighting its potential value for developing live attenuated vaccines or combined vaccine vectors. Our findings provide in-depth understanding of FAdV-4 pathogenesis and will support the development of novel FAdV-4 vaccines.

MATERIALS AND METHODS

Ethics statement. All animal studies were approved by the Committee on the Ethics of Animal Experiments of the Harbin Veterinary Research Institute (HVRI), Chinese Academy of Agricultural Sciences (HVRI-IACUC-2020-016). SPF chickens were purchased from the Experimental Animal Centre of HVRI and housed in negative pressure isolators with adequate food and light. All animal procedures were performed according to international standards on animal welfare.

Cell culture and viruses. Chicken LMH cells (ATCC CRL-2117) and CEL cells (prepared using 14-day-old SPF chicken embryos) were cultured at 37°C in a Dulbecco modified Eagle medium/nutrient mixture Ham F-12 (DMEM/F12; Sigma-Aldrich, USA) supplemented with 10% fetal bovine serum (FBS) (Sigma-Aldrich, USA), 100 IU/ml penicillin, and 100 μg/ml streptomycin in a 5% CO_2 atmosphere.

The highly pathogenic novel FAdV-4, HLJFAd15 (GenBank accession no. KU991797), was isolated as previously described (21). rWT-EGFP and rHN20-EGFP reporter viruses were constructed by inserting an enhanced green fluorescent protein (EGFP) expression cassette into rWT-FAdV4 and rHN20 backbones. Other recombinant viruses were constructed in this study. All viruses were propagated in LMH cells and stored at −80°C after isolation.

Construction of recombinant FAdV-4 fosmids. The HLJFAd15 fosmid infection clone was generated using a CopyControl fosmid library production kit (Epicentre, USA) according to the manufacturer's instructions. Recombinant FAdV-4 fosmids were generated by two-step Red/ET-mediated recombination using a Counter Selection BAC modification kit (Gene Bridges, USA). To generate chimeric fosmids replacing the hexon or fiber-2 genes, the hexon and fiber-2 genes of the nonpathogenic FAdV-4 strain ON1 (GenBank accession no. GU188428) were synthesized and cloned into pCAGGS vectors before recombination. In the first recombination step, the antibiotic selection cassette (rpsL-neo) was amplified using PCR with specific primers with 50-bp homology arms (Table 1). The PCR products were electro-transferred into DH10B electrocompetent cells containing the pRed/ET plasmid and HLJFAd15 fosmid to replace the hexon or fiber-2 genes. In the second recombination step, the hexon and fiber-2 genes of the ON1 strain were PCR amplified using the primers listed in Table 1 and electrotransferred into rpsL-neo-positive electrocompetent cells. To mutate the hexon protein, 13 single point mutations in hexon/HLJFAd15 and the I188R point mutation in hexon/ON1 were introduced by point mutation PCR in the pCAGGS vector using the primers in Table 2. Using these plasmids as the templates and hexon-insert F and hexon-insert R as primers, the mutated hexon gene was amplified using PCR and electrotransferred into the rpsL-neo-positive electrocompetent cells generated in step 1 to replace rpsL-neo. All recombinant fosmids were sequenced (Jilin Comate Bioscience Co., Ltd., Changchun, China) to confirm the correct sequence.

Rescue of recombinant viruses. Purified FAdV-4 fosmids were linearized by digestion with FseI (Thermo Scientific, Lithuania) and recovered by ethanol precipitation to release viral DNA. Next, 2 μg of DNA was transfected into LMH cells grown in 6-well plates using X-treme GENE HP DNA Reagent

TABLE 1 Primers used for construction of recombinant FAdV-4

Primer[a]	Sequence (5′–3′)[b]	Purpose
fiber2-rpsL F	TCCTATCCCTTTTTCCTATCAGGGTTACGTCTACTCCCCCAACGGGAACAGGCCTGGTGATGATGGCGGGATCG	Fiber-2 replacement
fiber2-rpsL R	GCAATCAACGTTCATGACTCTTTATTTGACACGCGGTGGGGAGGGCGCGCTCAGAAGAACTCGTCAAGAAGGCG	Fiber-2 replacement
fiber2-insert F	TCCTATCCCTTTTTCCTATCAGGGTTACGTCTACTCCCCCAACGGGAACAATGCTCCGAGCCCCTAAAAGAAGAC	Fiber-2 replacement
fiber2-insert R	GCAATCAACGTTCATGACTCTTTATTTGACACGCGGTGGGGAGGGCGCGCTTACGGGACGGAGGCCGCTGGAC	Fiber-2 replacement
hexon-rpsL F	CACGGCTTACAACCCGCTGGCTCCCAAGGAGTCCATGTTTAACAACTGGTGGCCTGGTGATGATGGCGGGATCG	Hexon replacement
hexon-rpsL R	GTGTCGAACACGCCATAGAGCATGTACACGTAAGTGGGATCATCCATGGGTCAGAAGAACTCGTCAAGAAGGCG	Hexon replacement
hexon-insert F	CACGGCTTACAACCCGCTGGCTCCCAAGGAGTCCATGTTTAACAACTGGTCGGAGACGGCACCCGGGCAGAACG	Hexon replacement
hexon-insert R	GTGTCGAACACGCCATAGAGCATGTACACGTAAGTGGGATCATCCATGGGGTCGAGCTCGAAGTTGATGACCAT	Hexon replacement

[a]F, forward primer; R, reverse primer.
[b]Underlining indicates homology arms.

(Roche, Switzerland). When CPE visibly occurred (within 1 week), the culture was subjected to three rounds of freeze-thaw. The supernatant was then harvested and propagated. The rescued wild-type virus was named rWT-FAdV4, and the gene replacement recombinant viruses were named rHN20 and rFB2. The hexon mutation strains were named according to the locations of the relative amino acids. All rescued virus genomes were extracted using the AxyPrep body fluid viral DNA/RNA miniprep kit (Axygen, USA) according to the manufacturer's instructions for PCR amplification and sequencing at Jilin Comate Bioscience Co.

Viral titration. Viral titers were determined by PFU analysis. Each virus was diluted 10-fold with serum-free DMEM/F12 medium and inoculated in LMH cells for 1 h. The medium was removed, and the cells were washed and covered with DMEM-agarose containing 2% FBS. Six days later, the agarose cells were fixed with 4% paraformaldehyde, stained with crystal violet, and rinsed with tap water. The plaques were then counted, and the viral titers were calculated.

Virus growth curves. LMH cells were infected with each FAdV-4 virus at a multiplicity of infection (MOI) of 0.01. The infected cells and supernatants were harvested at 12, 24, 48, 72, 96, and 120 h postinfection. Plaque assays were used to calculate virus titers.

Pathogenicity analysis of rescue virus. Three-week-old SPF chickens were used to analyze the pathogenicity of each recombinant virus. Chickens were intramuscularly injected with 10^5 PFU of the indicated viruses and monitored daily for 1 week. The dead and euthanized chickens were dissected, and tissues were collected for viral load determination and histopathological examination.

Real-time PCR. The collected tissue samples or infected LMH cells were homogenized in phosphate buffer solution (PBS), and total DNA was extracted using AxyPrep body fluid viral DNA/RNA miniprep kits (Axygen, Jiangsu, China). FAdV-4 genome amplification was used as an indicator of viral DNA (50) and the chicken ovotransferrin gene (OVO) was used as the reference (51). Real-time PCR amplification was performed with Premix Ex Taq (probe qPCR; TaKaRa, Japan) and a QuantStudio 5 system (Applied Biosystems, USA). The final concentration was calculated in copy numbers per 10^6 cells. All samples were examined in triplicates.

Histopathological examination. The liver, spleen, and bursa tissues were collected from dead or euthanized chickens and fixed with 10% formalin. The fixed tissues were embedded in paraffin and sectioned for observation using light microscopy after hematoxylin-eosin staining.

Phylogenetic analysis and sequence alignment. Complete FAdV-4 hexon gene sequences were downloaded from the GenBank database (https://www.ncbi.nlm.nih.gov/). GenBank accession numbers are annotated in the phylogenetic trees. The phylogenetic trees were mapped using MEGA7 software (52), and the sequences were aligned using the MegAlign program of DNASTAR software (DNASTAR, Madison, WI).

Serum neutralization assays. Fresh SPF chicken serum was separated from whole blood and passed through a 0.22-μm filter. A total of 10 μl of rWT-EGFP and rHN20-EGFP reporter viruses were coincubated with serum-free DMEM/F12 media or fresh SPF chicken serum in different volume ratios for 60 min at 42°C. The viruses were then added to LMH cells seeded in 12-well culture plates. After incubation at 37°C for 60 min, the cells were washed, and the medium was replaced with fresh medium containing 2% FBS. The cells were then incubated for an additional 48 h. EGFP-positive cells were examined using fluorescence microscopy. The relative ratio of fluorescence positive cells was detected using flow cytometry and normalized to cell-free medium controls. Then, 10-μl portions of rWT-FAdV4, rHN20, rI188R, and rR188I were pretreated with 90 μl of SPF chicken serum or serum-free DMEM/F12 and used to infect LMH cells. CPE was examined using microscopy, and the viral load was determined.

Evaluation of protection by rR188I. Thirty-two-week-old chickens were randomly and equally divided into three groups. The experimental group was inoculated with 10^5 PFU rR188I, whereas the

TABLE 2 Primers used for amino acid mutation of FAdV-4 hexon

Primer[a]	Sequence (5′–3′)[b]	Template
S164T F	AACACGAGCACCaCCAAAGACACGACG	HLJFAd15 hexon
S164T R	CGTCGTGTCTTTGGtGGTGCTCGTGTT	HLJFAd15 hexon
R188I F	CAGGGACCCGGAAtAAATCCTCTGCGA	HLJFAd15 hexon
R188I R	TCGCAGAGGATTTaTTCCGGGTCCCTG	HLJFAd15 hexon
R193Q F	AATCCTCTGCGACaGGTACAAAACGCC	HLJFAd15 hexon
R193Q R	GGCGTTTTGTACCtGTCGCAGAGGATT	HLJFAd15 hexon
Q195E F	CTGCGACGGGTAgAAAACGCCAACACC	HLJFAd15 hexon
Q195E R	GGTGTTGGCGTTTTcTACCCGTCGCAG	HLJFAd15 hexon
D238N F	TACTGGATCATGaATAACACGGGCACC	HLJFAd15 hexon
D238N R	GGTGCCCGTGTTATtCATGATCCAGTA	HLJFAd15 hexon
T240A F	ATCATGGATAACgCGGGCACCAATTAC	HLJFAd15 hexon
T240A R	GTAATTGGTGCCCGcGTTATCCATGAT	HLJFAd15 hexon
N243E F	AACACGGGCACCgaaTACCTGGGAGCG	HLJFAd15 hexon
N243E R	CGCTCCCAGGTAttcGGTGCCCGTGTT	HLJFAd15 hexon
T263M F	TCGTACCCAGATACCATgGTCGTGCCGCCT	HLJFAd15 hexon
T263M R	AGGCGGCACGACcATGGTATCTGGGTACGA	HLJFAd15 hexon
V264I F	TCGTACCCAGATACCATAaTCGTGCCGCCT	HLJFAd15 hexon
V264I R	AGGCGGCACGAtTATGGTATCTGGGTACGA	HLJFAd15 hexon
A410T F	AACACCGCCGTGaCcAACGCCACTACC	HLJFAd15 hexon
A410T R	GGTAGTGGCGTTgGtCACGGCGGTGTT	HLJFAd15 hexon
I574V F	GGCGCCAGCATCgTCTACAACGAGGTG	HLJFAd15 hexon
I574V R	CACCTCGTTGTAGAcGATGCTGGCGCC	HLJFAd15 hexon
F797A F	AGCGGACAGCAGgCTAGTCAGGAAGCC	HLJFAd15 hexon
F797A R	GGCTTCCTGACTAGcCTGCTGTCCGCT	HLJFAd15 hexon
A842G F	GCCATCCAACCCGgACAGGTCCTCAGC	HLJFAd15 hexon
A842G R	GCTGAGGACCTGTcCGGGTTGGATGGC	HLJFAd15 hexon
I188R F	CAGGGACCCGGAAgAAATCCTCTGCGG	ON1 hexon
I188R R	CCGCAGAGGATTTcTTCCGGGTCCCTG	ON1 hexon

[a]F, forward primer; R, reverse primer.
[b]Lowercase letters indicate mutated nucleotides.

challenge and healthy control groups were inoculated with an equal volume of DMEM/F12. After 2 weeks, the experimental and challenge control chickens were challenged with a lethal FAdV4 dose (10^4 PFU/bird). Healthy controls were inoculated with DMEM/F12. The dead and euthanized chickens at 5 days postchallenge were dissected for observation. Tissues were collected for viral load determination and histopathological examination.

Statistical analysis. All data were analyzed with unpaired t tests using Prism (GraphPad Software, Inc.). $P < 0.05$ was considered statistically significant.

REFERENCES

1. Hess M. 2000. Detection and differentiation of avian adenoviruses: a review. Avian Pathol 29:195–206. https://doi.org/10.1080/03079450050045440.
2. Steer PA, Kirkpatrick NC, O'Rourke D, Noormohammadi AH. 2009. Classification of fowl adenovirus serotypes by use of high-resolution melting-curve analysis of the hexon gene region. J Clin Microbiol 47:311–321. https://doi.org/10.1128/JCM.01567-08.
3. Schachner A, Matos M, Grafl B, Hess M. 2018. Fowl adenovirus-induced diseases and strategies for their control: a review on the current global situation. Avian Pathol 47:111–126. https://doi.org/10.1080/03079457.2017.1385724.
4. Su Q, Hou L, Gao Y, Liu X, Cui Z, Chang S, Zhao P. 2020. Research note: molecular relationship of the fowl adenovirus serotype 4 isolated from the contaminated live vaccine and wild strains isolated in China, 2013–2018. Poult Sci 99:6643–6646. https://doi.org/10.1016/j.psj.2020.08.063.
5. Ren G, Wang H, Yan Y, Liu F, Huang M, Chen R. 2019. Pathogenicity of a fowl adenovirus serotype 4 isolated from chickens associated with hydro-pericardium-hepatitis syndrome in China. Poult Sci 98:2765–2771. https://doi.org/10.3382/ps/pez042.
6. Mase M, Hiramatsu K, Nishijima N, Iguchi H, Honda S, Hanyu S, Iseki H, Watanabe S. 2020. Fowl adenoviruses type 8b isolated from chickens with inclusion body hepatitis in Japan. Avian Dis 64:330–334. https://doi.org/10.1637/aviandiseases-D-20-00028.
7. Mohamed MHA, El-Sabagh IM, Abdelaziz AM, Al-Ali AM, Alramadan M, Lebdah MA, Ibrahim AM, Al-Ankari AS. 2018. Molecular characterization of fowl aviadenoviruses species D and E associated with inclusion body hepatitis in chickens and falcons indicates possible cross-species transmission. Avian Pathol 47:384–390. https://doi.org/10.1080/03079457.2018.1457769.
8. Wang J, Zaheer I, Saleemi MK, Qi X, Gao Y, Cui H, Li K, Gao L, Fayyaz A, Hussain A, Liu C, Zhang Y, Wang X, Pan Q. 2020. The first complete genome sequence and pathogenicity characterization of fowl adenovirus 11 from chickens with inclusion body hepatitis in Pakistan. Vet Microbiol 244:108670. https://doi.org/10.1016/j.vetmic.2020.108670.
9. Mirzazadeh A, Grafl B, Abbasnia M, Emadi-Jamali S, Abdi-Hachesoo B, Schachner A, Hess M. 2021. Reduced performance due to adenoviral gizzard erosion in 16-day-old commercial broiler chickens in Iran, confirmed

experimentally. Front Vet Sci 8:635186. https://doi.org/10.3389/fvets.2021.635186.

10. Okuda Y, Ono M, Shibata I, Sato S. 2004. Pathogenicity of serotype 8 fowl adenovirus isolated from gizzard erosions of slaughtered broiler chickens. J Vet Med Sci 66:1561–1566. https://doi.org/10.1292/jvms.66.1561.

11. Mirzazadeh A, Asasi K, Schachner A, Mosleh N, Liebhart D, Hess M, Grafl B. 2019. Gizzard erosion associated with fowl adenovirus infection in slaughtered broiler chickens in Iran. Avian Dis 63:568–576. https://doi.org/10.1637/aviandiseases-D-19-00069.

12. Michou AI, Lehrmann H, Saltik M, Cotten M. 1999. Mutational analysis of the avian adenovirus CELO, which provides a basis for gene delivery vectors. J Virol 73:1399–1410. https://doi.org/10.1128/JVI.73.2.1399-1410.1999.

13. François A, Eterradossi N, Delmas B, Payet V, Langlois P. 2001. Construction of avian adenovirus CELO recombinants in cosmids. J Virol 75:5288–5301. https://doi.org/10.1128/JVI.75.11.5288-5301.2001.

14. Francois A, Chevalier C, Delmas B, Eterradossi N, Toquin D, Rivallan G, Langlois P. 2004. Avian adenovirus CELO recombinants expressing VP2 of infectious bursal disease virus induce protection against bursal disease in chickens. Vaccine 22:2351–2360. https://doi.org/10.1016/j.vaccine.2003.10.039.

15. Ye J, Liang G, Zhang J, Wang W, Song N, Wang P, Zheng W, Xie Q, Shao H, Wan Z, Wang C, Chen H, Gao W, Qin A. 2016. Outbreaks of serotype 4 fowl adenovirus with novel genotype, China. Emerg Microbes Infect 5:e50. https://doi.org/10.1038/emi.2016.50.

16. Liu Y, Wan W, Gao D, Li Y, Yang X, Liu H, Yao H, Chen L, Wang C, Zhao J. 2016. Genetic characterization of novel fowl aviadenovirus 4 isolates from outbreaks of hepatitis-hydropericardium syndrome in broiler chickens in China. Emerg Microbes Infect 5:e117. https://doi.org/10.1038/emi.2016.115.

17. Pan Q, Liu L, Wang Y, Zhang Y, Qi X, Liu C, Gao Y, Wang X, Cui H. 2017. The first whole-genome sequence and pathogenicity characterization of a fowl adenovirus 4 isolated from ducks associated with inclusion body hepatitis and hydropericardium syndrome. Avian Pathol 46:571–578. https://doi.org/10.1080/03079457.2017.1311006.

18. Yu X, Wang Z, Chen H, Niu X, Dou Y, Yang J, Tang Y, Diao Y. 2018. Serological and pathogenic analyses of fowl adenovirus serotype 4 (FAdV-4) strain in Muscovy ducks. Front Microbiol 9:1163. https://doi.org/10.3389/fmicb.2018.01163.

19. Wei Z, Liu H, Diao Y, Li X, Zhang S, Gao B, Tang Y, Hu J, Diao Y. 2019. Pathogenicity of fowl adenovirus (FAdV) serotype 4 strain SDJN in Taizhou geese. Avian Pathol 48:477–485. https://doi.org/10.1080/03079457.2019.1625305.

20. Griffin BD, Nagy É. 2011. Coding potential and transcript analysis of fowl adenovirus 4: insight into upstream ORFs as common sequence features in adenoviral transcripts. J Gen Virol 92:1260–1272. https://doi.org/10.1099/vir.0.030064-0.

21. Pan Q, Liu L, Gao Y, Liu C, Qi X, Zhang Y, Wang Y, Li K, Gao L, Wang X, Cui H. 2017. Characterization of a hypervirulent fowl adenovirus 4 with the novel genotype newly prevalent in China and establishment of reproduction infection model of hydropericardium syndrome in chickens. Poult Sci 96:1581–1588. https://doi.org/10.3382/ps/pew431.

22. Pan Q, Wang J, Gao Y, Cui H, Liu C, Qi X, Zhang Y, Wang Y, Wang X. 2018. The natural large genomic deletion is unrelated to the increased virulence of the novel genotype fowl adenovirus 4 recently emerged in China. Viruses 10:494. https://doi.org/10.3390/v10090494.

23. Schachner A, Grafl B, Hess M. 2021. Spotlight on avian pathology: fowl adenovirus (FAdV) in chickens and beyond: an unresolved host-pathogen interplay. Avian Pathol 50:2–5. https://doi.org/10.1080/03079457.2020.1810629.

24. Garcia-Beltran WF, Lam EC, St Denis K, Nitido AD, Garcia ZH, Hauser BM, Feldman J, Pavlovic MN, Gregory DJ, Poznansky MC, Sigal A, Schmidt AG, Iafrate AJ, Naranbhai V, Balazs AB. 2021. Multiple SARS-CoV-2 variants escape neutralization by vaccine-induced humoral immunity. Cell 1842372–2383. https://doi.org/10.1016/j.cell.2021.03.013.

25. Rees-Spear C, Muir L, Griffith SA, Heaney J, Aldon Y, Snitselaar JL, Thomas P, Graham C, Seow J, Lee N, Rosa A, Roustan C, Houlihan CF, Sanders RW, Gupta RK, Cherepanov P, Stauss HJ, Nastouli E, Doores KJ, van Gils MJ, McCoy LE, SAFER Investigators. 2021. The effect of spike mutations on SARS-CoV-2 neutralization. Cell Rep 34:108890. https://doi.org/10.1016/j.celrep.2021.108890.

26. Dejnirattisai W, Zhou D, Ginn HM, Duyvesteyn HME, Supasa P, Case JB, Zhao Y, Walter TS, Mentzer AJ, Liu C, Wang B, Paesen GC, Slon-Campos J, López-Camacho C, Kafai NM, Bailey AL, Chen RE, Ying B, Thompson C, Bolton J, Fyfe A, Gupta S, Tan TK, Gilbert-Jaramillo J, James W, et al. 2021.

The antigenic anatomy of SARS-CoV-2 receptor binding domain. Cell 184:2183–2200. https://doi.org/10.1016/j.cell.2021.02.032.

27. Conradie AM, Bertzbach LD, Trimpert J, Patria JN, Murata S, Parcells MS, Kaufer BB. 2020. Distinct polymorphisms in a single herpesvirus gene are capable of enhancing virulence and mediating vaccinal resistance. PLoS Pathog 16:e1009104. https://doi.org/10.1371/journal.ppat.1009104.

28. Li K, Liu Y, Xu Z, Zhang Y, Luo D, Gao Y, Qian Y, Bao C, Liu C, Zhang Y, Qi X, Cui H, Wang Y, Gao L, Wang X. 2019. Avian oncogenic herpesvirus antagonizes the cGAS-STING DNA-sensing pathway to mediate immune evasion. PLoS Pathog 15:e1007999. https://doi.org/10.1371/journal.ppat.1007999.

29. Sun P, Cui N, Liu L, Su S, Cheng Z, Chen R, Li Y, Cui Z. 2020. Attenuation of a recombinant Marek's disease virus lacking the meq oncogene and evaluation on its immune efficacy against Marek's disease virus. Poult Sci 99:1939–1945. https://doi.org/10.1016/j.psj.2019.11.059.

30. Liao Y, Reddy SM, Khan OA, Sun A, Lupiani B. 2021. A novel effective and safe vaccine for prevention of Marek's disease caused by infection with a very virulent plus (vv+) Marek's disease virus. Vaccines (Basel) 9:159. https://doi.org/10.3390/vaccines9020159.

31. Pan Q, Wang J, Gao Y, Wang Q, Cui H, Liu C, Qi X, Zhang Y, Wang Y, Li K, Gao L, Liu A, Wang X. 2020. Identification of chicken CAR homology as a cellular receptor for the emerging highly pathogenic fowl adenovirus 4 via unique binding mechanism. Emerg Microbes Infect 9:586–596. https://doi.org/10.1080/22221751.2020.1736954.

32. Wang W, Liu Q, Li T, Geng T, Chen H, Xie Q, Shao H, Wan Z, Qin A, Ye J. 2020. Fiber-1, not Fiber-2, directly mediates the infection of the pathogenic serotype 4 fowl adenovirus via its shaft and knob domains. J Virol 94:e00954-20. https://doi.org/10.1128/JVI.00954-20.

33. Zou X, Rong Y, Guo X, Hou W, Yan B, Hung T, Lu Z. 2021. Fiber1, but not fiber2, is the essential fiber gene for fowl adenovirus 4 (FAdV-4). J Gen Virol 102. https://doi.org/10.1099/jgv.0.001559.

34. Xie Q, Wang W, Li L, Kan Q, Fu H, Geng T, Li T, Wan Z, Gao W, Shao H, Qin A, Ye J. 2021. Domain in fiber-2 interacted with KPNA3/4 significantly affects the replication and pathogenicity of the highly pathogenic FAdV-4. Virulence 12:754–765. https://doi.org/10.1080/21505594.2021.1888458.

35. Liu R, Zhang Y, Guo H, Li N, Wang B, Tian K, Wang Z, Yang X, Li Y, Wang H, Zhang Y, Fu J, Zhao J. 2020. The increased virulence of hypervirulent fowl adenovirus 4 is independent of fiber-1 and penton. Res Vet Sci 131:31–37. https://doi.org/10.1016/j.rvsc.2020.04.005.

36. Zhang Y, Liu R, Tian K, Wang Z, Yang X, Gao D, Zhang Y, Fu J, Wang H, Zhao J. 2018. Fiber2 and hexon genes are closely associated with the virulence of the emerging and highly pathogenic fowl adenovirus 4. Emerg Microbes Infect 7:199. https://doi.org/10.1038/s41426-018-0203-1.

37. Supasa P, Zhou D, Dejnirattisai W, Liu C, Mentzer AJ, Ginn HM, Zhao Y, Duyvesteyn HME, Nutalai R, Tuekprakhon A, Wang B, Paesen GC, Slon-Campos J, López-Camacho C, Hallis B, Coombes N, Bewley KR, Charlton S, Walter TS, Barnes E, Dunachie SJ, Skelly D, Lumley SF, et al. 2021. Reduced neutralization of SARS-CoV-2 B.1.1.7 variant by convalescent and vaccine sera. Cell 184:2201–2211. https://doi.org/10.1016/j.cell.2021.02.033.

38. Forero A, Tisoncik-Go J, Watanabe T, Zhong G, Hatta M, Tchitchek N, Selinger C, Chang J, Barker K, Morrison J, Berndt JD, Moon RT, Josset L, Kawaoka Y, Katze MG. 2015. The 1918 influenza virus PB2 protein enhances virulence through the disruption of inflammatory and Wnt-mediated signaling in mice. J Virol 90:2240–2253. https://doi.org/10.1128/JVI.02974-15.

39. Nunes BTD, Fontes-Garfias CR, Shan C, Muruato AE, Nunes JGC, Burbano RMR, Vasconcelos PFC, Shi PY, Medeiros DBA. 2020. Zika structural genes determine the virulence of African and Asian lineages. Emerg Microbes Infect 9:1023–1033. https://doi.org/10.1080/22221751.2020.1753583.

40. Sun M, Zhang L, Cao Y, Wang J, Yu Z, Sun X, Liu F, Li Z, Liu P, Su J. 2020. Basic amino acid substitution at residue 367 of the envelope protein of Tembusu virus plays a critical role in pathogenesis. J Virol 94:e00743-20. https://doi.org/10.1128/JVI.00743-20.

41. Xu C, Xu B, Wu Y, Yang S, Jia Y, Liang W, Yang D, He L, Zhu W, Chen Y, Yang H, Yu B, Wang D, Qiao C. 2020. A single amino acid at position 431 of the PB2 protein determines the virulence of H1N1 swine influenza viruses in mice. J Virol 94:e00653-20. https://doi.org/10.1128/JVI.00653-20.

42. Waddington SN, McVey JH, Bhella D, Parker AL, Barker K, Atoda H, Pink R, Buckley SM, Greig JA, Denby L, Custers J, Morita T, Francischetti IM, Monteiro RQ, Barouch DH, van Rooijen N, Napoli C, Havenga MJ, Nicklin SA, Baker AH. 2008. Adenovirus serotype 5 hexon mediates liver gene transfer. Cell 132:397–409. https://doi.org/10.1016/j.cell.2008.01.016.

43. Kalyuzhniy O, Di Paolo NC, Silvestry M, Hofherr SE, Barry MA, Stewart PL, Shayakhmetov DM. 2008. Adenovirus serotype 5 hexon is critical for virus infection of hepatocytes in vivo. Proc Natl Acad Sci U S A 105:5483–5488. https://doi.org/10.1073/pnas.0711757105.

44. Doronin K, Flatt JW, Di Paolo NC, Khare R, Kalyuzhniy O, Acchione M, Sumida JP, Ohto U, Shimizu T, Akashi-Takamura S, Miyake K, MacDonald JW, Bammler TK, Beyer RP, Farin FM, Stewart PL, Shayakhmetov DM. 2012. Coagulation factor X activates innate immunity to human species C adenovirus. Science 338:795–798. https://doi.org/10.1126/science.1226625.

45. Bottermann M, Foss S, Caddy SL, Clift D, van Tienen LM, Vaysburd M, Cruickshank J, O'Connell K, Clark J, Mayes K, Higginson K, Lode HE, McAdam MB, Sandlie I, Andersen JT, James LC. 2019. Complement C4 prevents viral infection through capsid inactivation. Cell Host Microbe 25:617–629. https://doi.org/10.1016/j.chom.2019.02.016.

46. Xu Z, Qiu Q, Tian J, Smith JS, Conenello GM, Morita T, Byrnes AP. 2013. Coagulation factor X shields adenovirus type 5 from attack by natural antibodies and complement. Nat Med 19:452–457. https://doi.org/10.1038/nm.3107.

47. Zhu FC, Li YH, Guan XH, Hou LH, Wang WJ, Li JX, Wu SP, Wang BS, Wang Z, Wang L, Jia SY, Jiang HD, Wang L, Jiang T, Hu Y, Gou JB, Xu SB, Xu JJ, Wang XW, Wang W, Chen W. 2020. Safety, tolerability, and immunogenicity of a recombinant adenovirus type-5 vectored COVID-19 vaccine: a dose-escalation, open-label, non-randomised, first-in-human trial. Lancet 395:1845–1854. https://doi.org/10.1016/S0140-6736(20)31208-3.

48. Zhu FC, Hou LH, Li JX, Wu SP, Liu P, Zhang GR, Hu YM, Meng FY, Xu JJ, Tang R, Zhang JL, Wang WJ, Duan L, Chu K, Liang Q, Hu JL, Luo L, Zhu T, Wang JZ, Chen W. 2015. Safety and immunogenicity of a novel recombinant adenovirus type-5 vector-based Ebola vaccine in healthy adults in China: preliminary report of a randomised, double-blind, placebo-controlled, phase 1 trial. Lancet 385:2272–2279. https://doi.org/10.1016/S0140-6736(15)60553-0.

49. Guo Q, Chan JF, Poon VK, Wu S, Chan CC, Hou L, Yip CC, Ren C, Cai JP, Zhao M, Zhang AJ, Song X, Chan KH, Wang B, Kok KH, Wen Y, Yuen KY, Chen W. 2018. Immunization with a novel human type 5 adenovirus-vectored vaccine expressing the premembrane and envelope proteins of Zika virus provides consistent and sterilizing protection in multiple immunocompetent and immunocompromised animal models. J Infect Dis 218:365–377. https://doi.org/10.1093/infdis/jiy187.

50. Pan Q, Yang Y, Shi Z, Liu L, Gao Y, Qi X, Liu C, Zhang Y, Cui H, Wang X. 2017. Different dynamic distribution in chickens and ducks of the hypervirulent, novel genotype fowl adenovirus serotype 4 recently emerged in China. Front Microbiol 8:1005. https://doi.org/10.3389/fmicb.2017.01005.

51. Baigent SJ, Petherbridge LJ, Howes K, Smith LP, Currie RJ, Nair VK. 2005. Absolute quantitation of Marek's disease virus genome copy number in chicken feather and lymphocyte samples using real-time PCR. J Virol Methods 123:53–64. https://doi.org/10.1016/j.jviromet.2004.08.019.

52. Kumar S, Stecher G, Tamura K. 2016. MEGA7: Molecular Evolutionary Genetics Analysis version 7.0 for bigger datasets. Mol Biol Evol 33:1870–1874. https://doi.org/10.1093/molbev/msw054.